Mendeleev Communications

Mendeleev Commun., 2025, **35**, 183–186

Photosensitizing effect of benzene oxidation intermediates on the action spectra of Bi_2WO_6/TiO_2-N composites

Maria E. Morozova,[a,b] Mikhail N. Lyulyukin,*[a,b] Dmitry S. Selishchev[a,b] and Denis V. Kozlov[a,b]

[a] *G. K. Boreskov Institute of Catalysis, Siberian Branch of the Russian Academy of Sciences, 630090 Novosibirsk, Russian Federation. E-mail: lyulyukin@catalysis.ru*

[b] *Novosibirsk State University, 630090 Novosibirsk, Russian Federation*

DOI: 10.71267/mencom.7601

The dependence of the photonic efficiency on the wavelength, *i.e.* the action spectrum, was established for the test reactions of benzene and cyclohexane oxidation over the Bi_2WO_6/TiO_2-N composites and individual components. It was found that the action spectrum curve for cyclohexane oxidation reproduces the light absorption curve, while that for benzene oxidation indicates some additional activity in the range of 400–550 nm. It was concluded that the intermediate products of benzene oxidation on the catalyst surface exert a photosensitization effect, which significantly increases the photoactivity of Bi_2WO_6/TiO_2-N composites in the visible range.

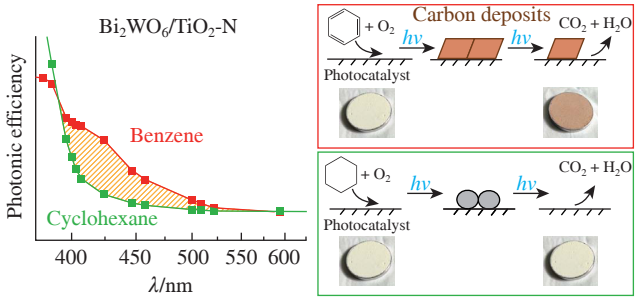

Keywords: TiO_2, Bi_2WO_6, composite, benzene, cyclohexane, action spectrum, oxidation.

In recent decades, scientific developments have been aimed at creating technologies that can manipulate inexhaustible, so-called alternative, energy sources such as sunlight. Photocatalysis is a promising technology that can help convert sunlight energy into energy for chemical reactions. One of the applications of photocatalysis that is currently being implemented in practice is photocatalytic degradation by oxidation.[1–7] The technology of photocatalytic oxidation of low-concentration VOCs in an oxygen-containing atmosphere under mild environmental conditions leads to the elimination of VOCs and a reduction in the hazard to the environment and human health.[8,9]

Researchers are developing methods to synthesize TiO_2 (the best-known and most active UV photocatalyst for oxidation) and other semiconductors with reduced band gap energy that can be activated by visible light.[10,11] It is known that the properties of semiconductor materials can be tuned by creating bulk or surface defects, or both.[12] In this case, due to impurity levels, N-doped TiO_2 (TiO_2-N) can not only absorb visible light but also act as a catalyst for chemical reactions.[13,14] However, due to internal processes, its activity can decrease due to the interaction of photogenerated charges with integrated defects until it loses the ability to absorb visible light.[14] To stabilize the photocatalytic activity, heterojunctions are created by coupling several semiconductors together. This allows for spatial separation of photoexited electron–hole pairs and provides increased stability and photoactivity compared to individual semiconductors.[15,16] For the efficient construction of such heterostructures, it is necessary to take into account such energy parameters as the position of the Fermi level, the position of the conduction band edge and the valence band of the components involved.[17] To enhance and stabilize the photocatalytic activity in the decomposition reaction of gaseous substances (acetone and benzene) under the action of visible light, TiO_2-N was combined with bismuth tungstate (Bi_2WO_6),[18] which reacts to visible light, as well as with other semiconductors for the decomposition of water contaminants such as 2,4-dichlorophenol[19] and 2,4-dinitrophenylhydrazine.[20] Among many air pollutants, benzene stands out for its persistence, high carcinogenicity and, therefore, a low threshold limit value.[9,21] So, the oxidation of benzene vapors, as well as other substances included in the BTEX list (benzene, toluene, ethylbenzene and xylenes), is an important object of research.[22,23]

The observed photoactivity of catalytic samples depends on many factors, which can be divided into light-independent and light-dependent groups. The first group includes the characteristics formed during the sample synthesis (phase composition and component content) and experimental study parameters, such as sample coating density, reaction component concentration, humidity and temperature. The second group includes radiation parameters, namely, the irradiated surface area, photon flux and photon energy distribution. The action spectrum is the dependence of photonic efficiency on the wavelength (*i.e.*, energy) of incident photons, where photonic efficiency is defined as the ratio of formed (or consumed) particles during the photocatalytic reaction per time unit.[24] The literature provides information on the comparison of the action spectrum and absorption spectrum of photocatalysts.[25] The absorption spectrum curve can predict the activity of a photocatalyst in certain processes, since it characterizes the energy transition processes associated with the absorption of light by the photocatalyst structure. On the one hand, the shape of the action spectrum curve may be similar to the absorption spectrum, which indicates that only photocatalytic processes occur due to excitation of the surface layer of the photocatalyst.[26] This type of action spectrum is called ‘ideal’ in the literature. On the other hand, these spectra may not be of the same pattern. A possible reason for this phenomenon is the presence of additional photosensitive side effects.[27,28] Therefore, in general, information from the action spectrum may be more useful for understanding the nature of the action of both modifying additives on the properties

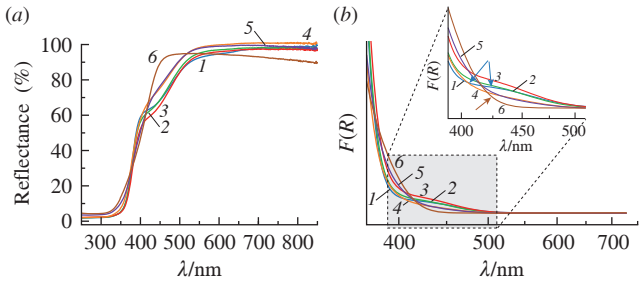

Figure 1 (*a*) Initial UV-VIS diffuse reflectance spectra and (*b*) Kubelka–Munk functions for (*1*) pristine TiO_2-N, (*6*) pure Bi_2WO_6 and Bi_2WO_6/TiO_2-N composites containing (*2*) 8, (*3*) 14, (*4*) 20 and (*5*) 30 wt% Bi_2WO_6. Blue arrows indicate the absorption shoulder due to nitrogen impurity.

of the catalyst and the process conditions on the observed photoresponse.

In this work, we measured the action spectra of Bi_2WO_6/TiO_2-N composites with a selected Bi_2WO_6 content. The focus of the study was to compare the action spectra of the composites during benzene and cyclohexane oxidation and to illustrate how the aromatic structure of the oxidized compound can affect the shape of the photoactivity dependence on the irradiation wavelength. This would be profound both for the investigation of processes occurring on the surface of the photocatalyst and for practical use.

The synthesis of the samples was performed according to the previously published methods.[14,29] The calculated bismuth tungstate contents of the considered composite samples were 8, 14, 20 and 30 wt%. All photocatalytic experiments in this study were performed in a continuous flow setup. Further experimental details are presented elsewhere[30–32] and can be found in Online Supplementary Materials, which also includes information on the photostability of the samples towards cyclohexane and benzene.

The UV-VIS diffuse reflectance spectroscopy data [Figure 1(*a*)] confirm that the UV absorption corresponds to the intrinsic absorption of the titanium dioxide structure. The blue shoulder of light absorption by pristine TiO_2-N and composites is observed due to the presence of an impurity nitrogen level [Figure 1(*b*), shown by the blue arrow].[14] Bismuth tungstate absorbs light without any shoulders, demonstrating a single line corresponding to a band gap of 2.8 eV.[29] The absorption of light by all the studied composites has a transient character, and the severity and position of the inflections of the curves depend on the ratio of the components. However, they all lie close to each other and differ insignificantly, by no more than 5–10% of the difference in light absorption.

It is known that during oxidation of benzene at a high concentration in air, the photocatalyst is usually deactivated by intermediate products of benzene oxidation, and the rate of accumulation of the final products is significantly reduced.[33] However, such deactivation is not observed during oxidation of cyclohexane, which is a cyclic hydrocarbon close in composition to benzene. Therefore, in this work, the focus is on the comparison of the action spectra of photocatalysts during oxidation of benzene and cyclohexane in order to understand in which region of the spectrum this effect is most noticeable.

Figure 2 shows the dependence of photonic efficiency on wavelength for photocatalysts selected for the oxidation reaction of benzene and cyclohexane vapors. Since cyclohexane is known to be oxidized faster, photonic efficiency during oxidation is generally higher for cyclohexane than for benzene.[9] Such a noticeable difference can arise due to different rates of charge recombination caused by differences in the structure of the molecules and their intermediates.

Removing the scale factor from consideration, the most important difference between the obtained action spectra becomes noticeable, which consists in the different positions of their lines for different composites. Thus, during the oxidation of cyclohexane, the

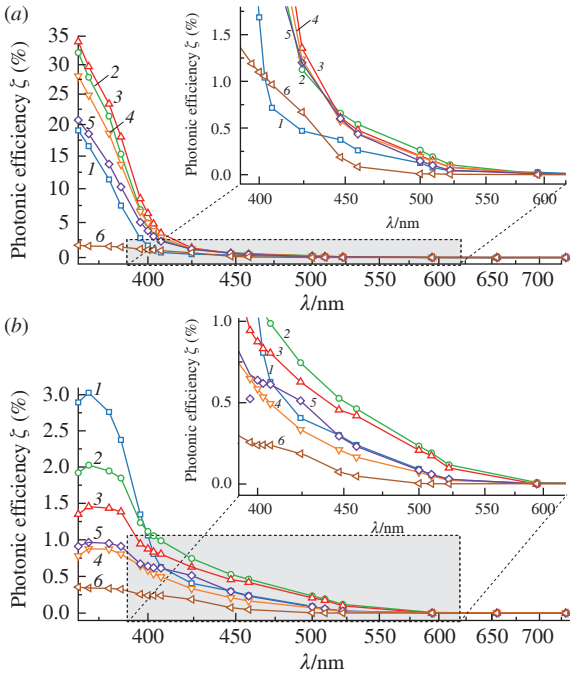

Figure 2 Action spectra of (*1*) pristine TiO_2-N, (*6*) pure Bi_2WO_6 and Bi_2WO_6/TiO_2-N composites containing (*2*) 8, (*3*) 14, (*4*) 20 and (*5*) 30 wt% Bi_2WO_6 during the photocatalytic oxidation of (*a*) cyclohexane and (*b*) benzene.

composites exhibit similar activity [Figure 2(*a*)] in the wavelength range of 420–500 nm, which is higher than the activity of each individual component of the composite in the entire wavelength range. At the same time, a shoulder is observed in the action spectrum of TiO_2-N, which was previously noted in the optical absorption spectrum. During the oxidation of benzene [Figure 2(*b*)], this shoulder is not observed, and the curves of the action spectra become flatter. In a numerical description, this means that the activity at the same points becomes higher than it could be for a spectrum proportionally changed relative to cyclohexane. So, in the visible region, an increased activity of composites relative to pristine nitrogen-doped titania is observed, but in the UV region their activity becomes significantly lower. This dependence is strikingly different from the picture observed during oxidation of cyclohexane vapors.

The selected action spectra of TiO_2-N and 30% Bi_2WO_6/TiO_2-N are presented in Figure 3 to show in detail the actual effect of the oxidized substance. For this purpose, the scales for the efficiencies are visually normalized to have the same value at 396 nm for both hydrocarbons. It can be seen that the oxidation of benzene under illumination with light in the 400–550 nm range for both photocatalysts results in a relative increase in their activity. When comparing the action spectra for the oxidation of cyclohexane vapor and the light absorption spectra, a clear similarity between the optical and action spectra is observed. This similarity is reflected in the presence of a shoulder at 450 nm for TiO_2-N and its absence for 30% Bi_2WO_6/TiO_2-N. Thus, the results indicate that the activity of the catalysts in cyclohexane vapor oxidation is directly related to the absorption and conversion of light by the catalyst structure.

In the case of benzene [see Figure 2(*b*)], a different picture is observed: the more titanium dioxide in the sample, the less the action spectrum during benzene oxidation resembles that during cyclohexane oxidation and, therefore, the absorption spectrum. This is clearly visible for the activity point at 424 nm, where the Bi_2WO_6 curve has a slight rise both in the absorption spectrum and in the action spectrum during cyclohexane oxidation. This rise in activity continues to exist for the 30% Bi_2WO_6/TiO_2-N sample, confirming its transient nature. It was previously shown[17,28] that

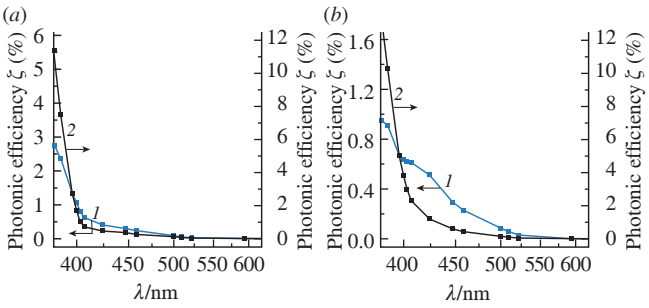

Figure 3 Comparison of action spectrum curves for (*a*) TiO_2-N and (*b*) 30% Bi_2WO_6/TiO_2-N during the oxidation of (*1*) benzene and (*2*) cyclohexane.

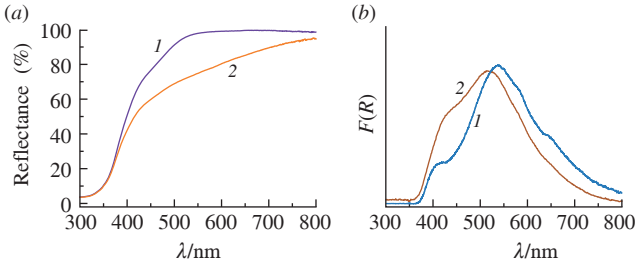

Figure 4 (*a*) UV-VIS diffuse reflectance spectra of 30% Bi_2WO_6/TiO_2-N composite (*1*) before and (*2*) after benzene oxidation reaction, measured relative to PTFE. (*b*) Kubelka–Munk functions of (*1*) TiO_2-N and (*2*) 30% Bi_2WO_6/TiO_2-N samples after benzene oxidation reaction, measured relative to the corresponding samples before the reaction.

at a lower bismuth tungstate content in the sample, titanium dioxide is not completely filled with the tungstate phase due to insufficient material for the complete formation of this phase. It is worth noting that the samples with 8 and 14% tungstate content demonstrate here noticeably higher activity in the visible range under the conditions used, which can be unambiguously attributed to the difference in the concentration of benzene vapors during the experiments and the reduced deactivation by intermediates. Visually, all samples changed their color after the experiment and acquired a brown hue.

According to published data, the benzene oxidation reaction occurs on the surface and is not accompanied by the release of a large amount of gaseous products.[33] The intermediates formed on the surface contain fragments of aromatic rings,[34,35] which may be the cause of the photosensitization effect. This can be indirectly confirmed by registering energy transitions. For this purpose, the diffuse reflectance spectra of the samples were recorded before and immediately after the reaction in the experimental setup [Figure 4(*a*)]. These diffuse reflectance spectra were measured using polytetrafluoroethylene (PTFE) as a standard. Such an operational procedure allows determining the relative change in light absorption. However, we proposed to use a recording procedure in which the diffuse reflectance of the sample under study is recorded relative to the sample before the reaction as a standard [Figure 4(*b*)]. Such measurement manipulations make it possible to more clearly demonstrate the change in absorption due to photooxidation processes. In general, the same result can be obtained mathematically if we consider that both spectra in Figure 4(*a*) were recorded relative to the same reference PTFE sample and recalculate the spectrum after the reaction using the spectrum before the reaction. In both cases, it can be said that any difference in the spectra can be unambiguously attributed to the presence of benzene oxidation intermediates on the catalyst surface and, accordingly, to the effect of light absorption by carbon deposits. In order to confirm the assumption about the change in the photocatalyst surface under the influence of carbon deposits, IR spectra were obtained for the TiO_2-N and 30% Bi_2WO_6/TiO_2-N samples after photooxidation of benzene and cyclohexane (see Online Supplementary Materials).

The absorption spectrum of the deposits on TiO_2-N was obtained in the same way, and both relative spectra for the TiO_2-N and 30% Bi_2WO_6/TiO_2-N samples are presented in Figure 4(*b*). The figure clearly illustrates that the absorption changes are noticeably different, which may indicate both a difference in the structure of the intermediates on the surface and a difference in their distribution deep in the layer due to the different morphology of the samples. The difference in the specific surface area, according to the data presented earlier,[29] is 17%. The absorption after cyclohexane oxidation is almost unchanged (see Online Supplementary Materials).

The absorption of incident radiation by the surface deposits occurs in a wide range of the visible spectrum, from 380 to 800 nm. It can be said that these deposits photosensitize the catalyst surface under visible light and allow the generation of a larger number of active species by the semiconductor structure or the LMCT phenomenon. Thus, it can be assumed that the aromatic structure of the carbon deposits on the surface increases the activity of the samples during the photocatalytic oxidation of benzene. This effect is known to be used in commercial visible light-sensitive photocatalysts such as KRONOS vlp7000© and KRONO*Clean*® 7000 from Kronos Worldwide Inc., which contain aromatic surface-supported species to enhance the sensitivity to visible light.[30,36–38] Sensitization through adsorbed aromatic compounds is also known to be used for adsorption-controlled selective oxidation in liquid media.[39–41] However, as with any 'dopant', the positive effect is limited. As the amount of deposits increases, more visible light can be absorbed. However, this light is absorbed by the deposits on the surface and partially blocks the active centers. This also results in surface shielding and a decrease in the overall reaction rate due to less efficient charge transfer from the deposits to the catalyst.

In conclusion, we have found that the action spectra of TiO_2-N, Bi_2WO_6 and their composites during the oxidation of benzene and cyclohexane differ both numerically and in the shape of the curves. Comparison of the action spectra with the optical absorption spectra made it possible to understand that in the case of benzene oxidation, the surface photosensitization occurs due to the carbon deposits formed during the process. The amount of these deposits was determined for the selected TiO_2-N and 30% Bi_2WO_6/TiO_2-N samples and turned out to be comparable, about 1.4 mg of carbon per sample. To illustrate their effect on the absorption spectra, absorbance was recorded using a non-irradiated catalyst sample as a reference standard. The absorption spectra obtained in this way for the surface carbon deposits differ, which indicates both potentially different forms of deposits and their different effects. This observed effect of 'selfphotosensitization' can be used to enhance the absorption of light in a wide spectral range (*e.g.*, solar radiation), which is currently considered as a trend[42] in the development of photocatalytic technologies and their practical application. This aspect deserves a separate study using an expanded set of methods. Finally, the work performed has once again demonstrated that obtaining action spectra is a powerful method for analyzing the activity of photocatalysts, allowing one to analyze the correlation of their activity in different ranges. It has the potential for practical application in the case of using radiation from broadband artificial light sources and solar radiation.

This work was supported by the Russian Science Foundation (project no. 23-23-00505, https://rscf.ru/project/23-23-00505/).

Online Supplementary Materials

Supplementary data associated with this article can be found in the online version at doi: 10.71267/mencom.7601.

References

1 S. Almaie, V. Vatanpour, M. H. Rasoulifard and I. Koyuncu, *Chemosphere*, 2022, **306**, 135655; https://doi.org/10.1016/j.chemosphere.2022.135655.
2 E. David and V.-C. Niculescu, *Int. J. Environ. Res. Public Health*, 2021, **18**, 13147; https://doi.org/10.3390/ijerph182413147.
3 G. Masresha, S. A. Jabasingh, S. Kebede, D. Doo-Arhin and M. Assefa, *Can. J. Chem. Eng.*, 2023, **101**, 6905; https://doi.org/10.1002/cjce.24978.
4 M. Surana, D. S. Pattanayak, V. Yadav, V. K. Singh and D. Pal, *Environ. Res.*, 2024, **247**, 118268; https://doi.org/10.1016/j.envres.2024.118268.
5 M. F. Lanjwani, M. Tuzen, M. Y. Khuhawar and T. A. Saleh, *Inorg. Chem. Commun.*, 2024, **159**, 111613; https://doi.org/10.1016/j.inoche.2023.111613.
6 F. Huang, X. Zhang, Y. Chang, W. Chen, H. Wu, L. Li and J. Jia, *Mol. Catal.*, 2024, **556**, 113928; https://doi.org/10.1016/j.mcat.2024.113928.
7 B. Borjigin, L. Ding, C. Liu, H. Li and X. Wang, *Chem. Eng. J.*, 2024, **485**, 149995; https://doi.org/10.1016/j.cej.2024.149995.
8 Y. Zhang, Y. Wang, R. Xie, H. Huang, M. K. H. Leung, J. Li and D. Y. C. Leung, *Environ. Sci. Technol.*, 2022, **56**, 16582; https://doi.org/10.1021/acs.est.2c05444.
9 M. N. Lyulyukin, P. A. Kolinko, D. S. Selishchev and D. V. Kozlov, *Appl. Catal., B*, 2018, **220**, 386; https://doi.org/10.1016/J.APCATB.2017.08.020.
10 Ö. Kerkez-Kuyumcu, E. Kibar, K. Dayıoğlu, F. Gedik, A. N. Akın and Ş. Özkara-Aydınoğlu, *J. Photochem. Photobiol., A*, 2015, **311**, 176; https://doi.org/10.1016/j.jphotochem.2015.05.037.
11 A. V. Shtareva, D. S. Shtarev, M. I. Balanov, V. O. Krutikova and I. A. Astapov, *Russ. J. Inorg. Chem.*, 2022, **67**, 1375; https://doi.org/10.1134/ S0036023622090157.
12 M. V. Korolenko, P. B. Fabritchnyi, Y. A. Teterin, K. I. Maslakov and M. I. Afanasov, *Mendeleev Commun.*, 2024, **34**, 440; https://doi.org/10.1016/j.mencom.2024.04.041.
13 A. Fujishima, X. Zhang and D. A. Tryk, *Surf. Sci. Rep.*, 2008, **63**, 515; https://doi.org/10.1016/j.surfrep.2008.10.001.
14 N. Kovalevskiy, D. Svintsitskiy, S. Cherepanova, S. Yakushkin, O. Martyanov, S. Selishcheva, E. Gribov, D. Kozlov and D. Selishchev, *Nanomaterials*, 2022, **12**, 4146; https://doi.org/10.3390/nano12234146.
15 Y. Zhao, X. Linghu, Y. Shu, J. Zhang, Z. Chen, Y. Wu, D. Shan and B. Wang, *J. Environ. Chem. Eng.*, 2022, **10**, 108077; https://doi.org/10.1016/j.jece.2022.108077.
16 H. Yang, *Mater. Res. Bull.*, 2021, **142**, 111406; https://doi.org/10.1016/j.materresbull.2021.111406.
17 Z. Wang, Z. Lin, S. Shen, W. Zhong and S. Cao, *Chin. J. Catal.*, 2021, **42**, 710; https://doi.org/10.1016/S1872-2067(20)63698-1.
18 N. Kovalevskiy, S. Cherepanova, E. Gerasimov, M. Lyulyukin, M. Solovyeva, I. Prosvirin, D. Kozlov and D. Selishchev, *Nanomaterials*, 2022, **12**, 359; https://doi.org/10.3390/nano12030359.
19 S. Bagwasi, Y. Niu, M. Nasir, B. Tian and J. Zhang, *Appl. Surf. Sci.*, 2013, **264**, 139; https://doi.org/10.1016/j.apsusc.2012.09.145.
20 S. Dong, S. Chen, F. He, J. Li, H. Li and K. Xu, *J. Alloys Compd.*, 2022, **908**, 164586; https://doi.org/10.1016/j.jallcom.2022.164586.
21 T.-D. Pham, B.-K. Lee and C.-H. Lee, *Appl. Catal., B*, 2016, **182**, 172; https://doi.org/10.1016/j.apcatb.2015.09.023.
22 K. Xie, D. Xu, C. Li, X. Liu, X. Hu, Z. Ma, X. Tang and Y. Chen, *Ind. Eng. Chem. Res.*, 2019, **58**, 17601; https://doi.org/10.1021/acs.iecr.9b03370.
23 M. N. Lyulyukin, N. S. Kovalevskiy, I. P. Prosvirin, D. S. Selishchev and D. V. Kozlov, *Mendeleev Commun.*, 2023, **33**, 497; https://doi.org/10.1016/j.mencom.2023.06.018.
24 S. E. Braslavsky, A. M. Braun, A. E. Cassano, A. V. Emeline, M. I. Litter, L. Palmisano, V. N. Parmon and N. Serpone, *Pure Appl. Chem.*, 2011, **83**, 931; https://doi.org/10.1351/PAC-REC-09-09-36.
25 R. Quesada-Cabrera, A. Mills and C. O'Rourke, *Appl. Catal., B*, 2014, **150–151**, 338; https://doi.org/10.1016/j.apcatb.2013.12.008.
26 R. Abe, H. Takami, N. Murakami and B. Ohtani, *J. Am. Chem. Soc.*, 2008, **130**, 7780; https://doi.org/10.1021/ja800835q.
27 T. Torimoto, N. Nakamura, S. Ikeda and B. Ohtani, *Phys. Chem. Chem. Phys.*, 2002, **4**, 5910; https://doi.org/10.1039/B207448F.
28 T. Watanabe, T. Takizawa and K. Honda, *J. Phys. Chem.*, 1977, **81**, 1845; https://doi.org/10.1021/j100534a012.
29 M. N. Lyulyukin, M. E. Morozova, D. A. Polskikh, I. P. Prosvirin, S. V. Cherepanova, D. S. Selishchev and D. V. Kozlov, *J. Struct. Chem.*, 2024, **65**, 341; https://doi.org/10.1134/S0022476624020124.
30 M. Lyulyukin, N. Kovalevskiy, D. Selishchev and D. Kozlov, *J. Photochem. Photobiol., A*, 2021, **405**, 112981; https://doi.org/10.1016/j.jphotochem.2020.112981.
31 M. N. Lyulyukin, N. S. Kovalevskiy, E. A. Fedorova, D. S. Selishchev and D. V. Kozlov, *Mendeleev Commun.*, 2022, **32**, 278; https://doi.org/10.1016/j.mencom.2022.03.042.
32 N. S. Kovalevskiy, M. N. Lyulyukin, D. V. Kozlov and D. S. Selishchev, *Mendeleev Commun.*, 2021, **31**, 644; https://doi.org/10.1016/j.mencom.2021.09.017.
33 D. V. Kozlov, *Theor. Exp. Chem.*, 2014, **50**, 133; https://doi.org/10.1007/s11237-014-9358-6.
34 H. Einaga, S. Futamura and T. Ibusuki, *Appl. Catal., B*, 2002, **38**, 215; https://doi.org/10.1016/S0926-3373(02)00056-5.
35 H. Einaga, S. Futamura and T. Ibusuki, *Phys. Chem. Chem. Phys.*, 1999, **1**, 4903; https://doi.org/10.1039/A906214I.
36 M. Lyulyukin, T. Filippov, S. Cherepanova, M. Solovyeva, I. Prosvirin, A. Bukhtiyarov, D. Kozlov and D. Selishchev, *Nanomaterials*, 2021, **11**, 1036; https://doi.org/10.3390/NANO11041036.
37 D. M. Tobaldi, M. P. Seabra, G. Otero-Irurueta, Y. R. de Miguel, R. J. Ball, M. K. Singh, R. C. Pullar and J. A. Labrincha, *RSC Adv.*, 2015, **5**, 102911; https://doi.org/10.1039/C5RA22816F.
38 D. S. Selishchev, T. N. Filippov, M. N. Lyulyukin and D. V. Kozlov, *Chem. Eng. J.*, 2019, **370**, 1440; https://doi.org/10.1016/j.cej.2019.03.280.
39 S. Higashimoto, K. Okada, M. Azuma, H. Ohue, T. Terai and Y. Sakata, *RSC Adv.*, 2012, **2**, 669; https://doi.org/10.1039/C1RA00417D.
40 S. Higashimoto, N. Suetsugu, M. Azuma, H. Ohue and Y. Sakata, *J. Catal.*, 2010, **274**, 76; https://doi.org/10.1016/j.jcat.2010.06.006.
41 A.-S. Paschke, D. Selishchev, M. Lyulyukin and D. Kozlov, *Mol. Catal.*, 2022, **524**, 112263; https://doi.org/10.1016/j.mcat.2022.112263.
42 D. Spasiano, R. Marotta, S. Malato, P. Fernandez-Ibañez and I. Di Somma, *Appl. Catal., B*, 2015, **170–171**, 90; https://doi.org/10.1016/j.apcatb.2014.12.050.

Received: 26th August 2024; Com. 24/7601